

Statistical Analysis of Ferroresonance Phenomena for 400 kV Double-Circuit Transmission Systems

R. Zhang, J.S. Peng, S.P. Ang, H.Y. Li, Z.D. Wang and P. Jarman

Abstract—Investigation of ferroresonance that can occur in a 400kV double-circuit transmission system is carried out in this paper, with consideration focusing on potential impacts of transmission line up-rating. The possible distribution range of inter-circuit capacitances is calculated in addition to the distribution range of magnetizing curve especially around the knee point area based on the test report database of 400kV transformers. Through conducting simulations with parameters in the distribution range, the frequency of occurrence of ferroresonance under different line and transformer combinations is obtained, showing that the chance of encountering sustained ferroresonance, if is not the same, does not increase significantly after transmission line up-rating.

Keywords: Statistical Analysis, Transformer, Ferroresonance.

I. INTRODUCTION

Driven by the growth of demand, it is forecasted that the system power capacity will continue to increase in the UK [1]. Most of the generated power is expected to be delivered to load centres through transmission overhead lines which are nowadays considered to be over saturated and reaching to their critical values of capacity and sag [2]. This may be relieved by building new transmission corridors. However, due to limited ground space as well as concerns over economic and environmental justifications, the permit to build new transmission lines is difficult to obtain. Therefore, increasing the power transfer capability of overhead lines through reinforcing existing transmission lines has become a more applicable option. This can be achieved by overhead line up-grading, up-rating and refurbishment [3].

In the UK, the configuration of 400kV double-circuit transmission system can have potential risks of ferroresonance. One example can be referred to a field test carried out in National Grid [4-5] which confirms that the $16^{2/3}$ Hz and the 50 Hz ferroresonance can be induced as a result of switching out one of the double-circuit lines connected to a non-loaded power transformer. Ferroresonance should be further

addressed when transmission lines are upgraded or up-rated, since this may significantly changed the inter-phase and inter-circuit spacing and increase the likelihood of ferroresonance and also its severity.

Ferroresonance is not specific to the UK transmission system, it was also reported in the USA where ferroresonance occurred in a transformer terminated line, due to an energized parallel line on the same right-of-way [6]. The work presented in this paper is the continuation of the previous work published in [7]. It makes further investigation on the inter-circuit capacitances when they are modified by up-rating of existing transmission lines. In addition, the study also considers the possible variation of transformer magnetizing characteristics. The statistical range of inter-circuit coupling capacitors and that of transformer magnetizing characteristics are determined first. Simulation was carried out to identify the critical combination of line and transformer that may increase the severity and likelihood of ferroresonance.

II. STATISTICAL DETERMINATION OF SYSTEM PARAMETERS

A. Ferroresonance Phenomenon

Ferroresonance is one of the main transient issues in distribution and transmission systems. In general it can occur in a lossless electric circuit which contains interaction between capacitor and non-linear inductance. It may cause expensive equipment failure and reduce system reliability. Field measurements on power systems, experimental tests conducted on system models, together with numerical simulations, enable classification of ferroresonance in different modes, including fundamental mode (FM), sub-harmonic mode (SM), chaotic mode (CM) and quasi-periodic mode (QM) [8]. In the case when the ferroresonance is not sustained, it is considered as decay mode (DM). It is more harmful when the system is locked into FM due to higher overvoltages and overcurrents, and therefore it is normally of main concern.

Fig. 1 shows the single-line arrangement of a typical 400 kV double-circuit transmission system.

This work was supported in part by National Grid, UK.

R. Zhang, J.S. Peng, H.Y. Li, Z.D. Wang are with School of Electrical and Electronic Engineering at the University of Manchester, Manchester, M13 9PL, U.K. (Email: rui.zhang@postgrad.manchester.ac.uk, jinsheng.peng@postgrad.manchester.ac.uk, haiyu.li@manchester.ac.uk, Corresponding author: zhongdong.wang@manchester.ac.uk).

S.P. Ang is with Institute Technology Brunei. He was formerly a PhD student at the University of Manchester UK where this piece of research work was conducted. (Email: Spang@itb.edu.bn).

P. Jarman is with National Grid, Warwick Technology Park, Gallows Hill, Warwick CV34 6DA UK (Email: paul.jarman@uk.ngrid.com).

Paper submitted to the International Conference on Power Systems Transients (IPST2011) in Delft, the Netherlands June 14-17, 2011

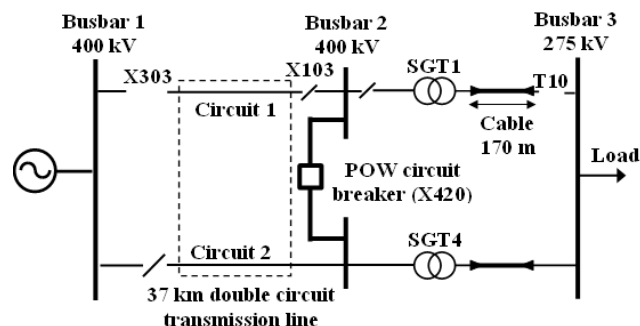


Fig. 1. Single-line diagram of 400 kV transmission system

The short-circuit level of the upstream network is 20 GVA. The line is un-transposed, with a length of 37 km. It is terminated with two three-phase power transformers: one is 1000MVA (SGT1) and the other is 180MVA (SGT4); both of them are autotransformer (400/275/13kV) with vector group of YNa0d1. The occurrence of FM and SM has been recorded when a series of switching operation was carried out in the following way:

1. Prior to the operation, the disconnector X_{303} and the circuit breaker T_{10} are opened. All the other disconnectors and circuit breaker X_{420} connecting to busbar 2 are in service.
2. The circuit is reconfigured by opening circuit breaker X_{420} . This operation will form a circuit consisting of voltage source connected to SGT1 via the coupling capacitances of double circuit transmission line.

In this typical double-circuit system, the initiation of ferroresonance is essentially caused by the interaction between the non-linear magnetizing inductance in the transformer and the line capacitances. This interaction could be complicated by the variation of system parameters. For example, between transmission lines building on a specific tower, the inter-circuit capacitances can be varied due to the change of sag, impacts of weather and load variation.

In the future the increasing power transfer capacity requires reinforcement of transmission lines, and more power transformers due to aging will be put into asset replacement schedule. Different applications and selections will result in different line and transformer combinations. These factors should be proactively taken into account to design a system less susceptible to ferroresonance.

B. Statistical Analysis of Line Parameters

1) Different Tower Dimension

The three typical 400kV double-circuit transmission line structure used by National Grid are represented by line 1, line 2 and line 3, as shown in Fig. 2 [9]. The geometrical distances between conductors and between conductor and ground will be used for calculating inter-circuit capacitances.

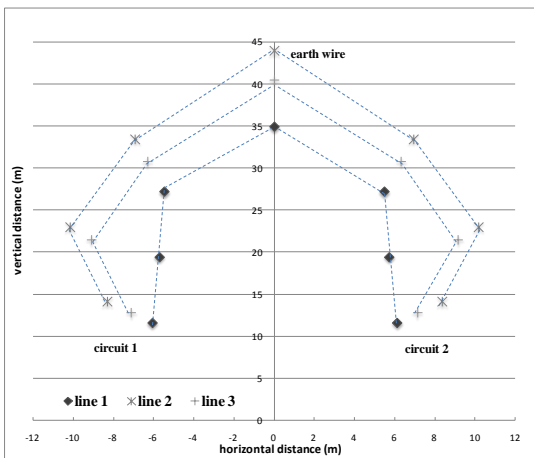


Fig. 2. Physical dimensions of 400 kV double-circuit transmission lines

2) Geometrical Variations

Upgrading of existing transmission lines can include increasing either thermal or voltage rating, and here we only

consider the scenario of thermal uprating. This could include adjusting conductor attachment height, re-tensioning, re-conducting or the possible use of composite cross-arm [10]. All of these will not bring fundamental change to the basic dimension of the tower; however minor geometric changes do exist. In this paper the possible geometric variation range in terms of horizontal and vertical distances are studied. As illustrated in Fig. 3, it is assumed that the horizontal distance varies within $\pm 10\%$ of the original value, and the vertical variation is between everyday sag and maximum sag.

Taking one pair of transmission line as an example, which is shown in Fig. 3, the transmission line with everyday sag and original horizontal distance was defined as the base case. The sag was then varied from everyday sag to maximum sag by three equivalent steps. The horizontal distance was varied within the range of $\pm 10\%$ of the original distance with a step change of 5%.

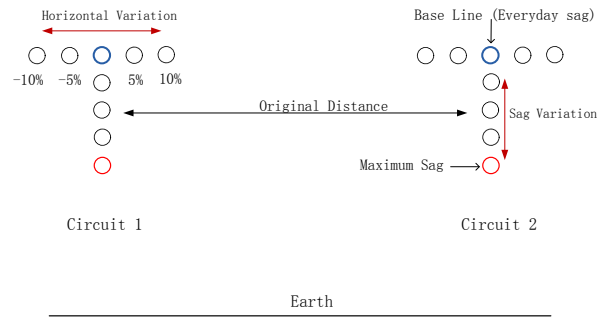


Fig. 3. Variation of horizontal distance and sag

3) Determination of Coupling Capacitances

The inter-circuit capacitance matrix $[C]$ is obtained by the inverse of the Maxwell's coefficient matrix $[P]$ given as:

$$[C] = inv[P] \quad (1)$$

The diagonal elements P_{ii} of matrix $[P]$ can be calculated by (2) and the off-diagonal elements P_{ik} can be deduced from (3).

$$P_{ii} = \frac{1}{2\pi\epsilon_0} \ln\left(\frac{2h_i}{r_i}\right) \quad (2)$$

$$P_{ik} = P_{ki} = \frac{1}{2\pi\epsilon_0} \left(\frac{D_{ik}}{d_{ik}}\right) \quad (3)$$

where:

- h_i = average height above ground of conductor i ;
- r_i = radius of conductor i ;
- D_{ik} = distance between conductor i and image conductor k ;
- d_{ik} = distance between conductor i and k ;
- ϵ_0 = permittivity of free space

Given the inputs of n scenarios of geometrical variation, n $[C]$ matrixes can be generated using (1), (2) and (3). Therefore, each inter-circuit capacitance, originated from $[C]$, has n samples. These samples form the distribution for each inter-

circuit capacitance c_i . Standard deviation and probability density function can be used to address these distributions. Firstly, the C_{mean} which is the arithmetic mean of all the samples should be estimated using (4):

$$C_{mean} = \frac{1}{n} \sum_{i=1}^n c_i \quad (4)$$

Then, to address the property of each distribution, the spread of the distribution is measured by standard deviation calculated using (5):

$$\sigma = \sqrt{\frac{1}{n} \sum_{i=1}^n (c_i - c_{mean})^2} \quad (5)$$

This standard deviation is combined with the arithmetic mean value to deduce the probability density function (PDF) using (6):

$$PDF = \frac{1}{\sqrt{2\pi\sigma^2}} e^{-\frac{1}{2} \left(\frac{c_i - c_{mean}}{\sigma} \right)^2} \quad (6)$$

C. Statistical Analysis of Transformer Magnetizing Characteristics

Transformer saturation characteristics should be correctly represented, especially for the knee point area, which accounts for the modelling accuracy of ferroresonance studies [11]. However, in the UK, the transformer age varies from 40 years old to brand new. Refinement of core material and change of structure design has resulted in changes of transformer saturation characteristics.

In order to identify the possible pattern of transformer saturation characteristics, a statistical analysis of the transformer open-circuit test data was performed. The transmission transformers considered here include two types: 750MVA and 1000MVA autotransformers. Fig. 4 and Fig. 5 show the mapping of open-circuit test data, which include 12 units of 750MVA transformers and 25 units of 1000MVA transformers, respectively. It should be noted that, for all units included in the database, the open-circuit tests were carried out with 90%, 100% and 110% rated voltage.

The mapping provides detail description of the magnetizing characteristic shape around the knee point area. It can be seen that: at 90% rated voltage, the working points for all the available transformer units are nearly the same; at 100% rated voltage, the working points start to deviate, with older transformers showing a step change of magnetizing current than the new; at 110% rated voltage, the deviation between new and older transformers in terms of their magnetization characteristics become even more significant.

Although the available test data cannot give estimation on the deeper saturation behaviour, it indicates that the saturation characteristics of a typical transformer should be described with a range rather than an individual case.

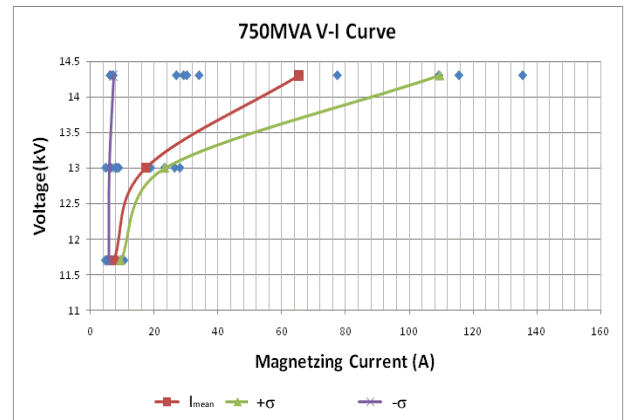


Fig. 4. Mapping open-circuit test data of 750MVA transformers

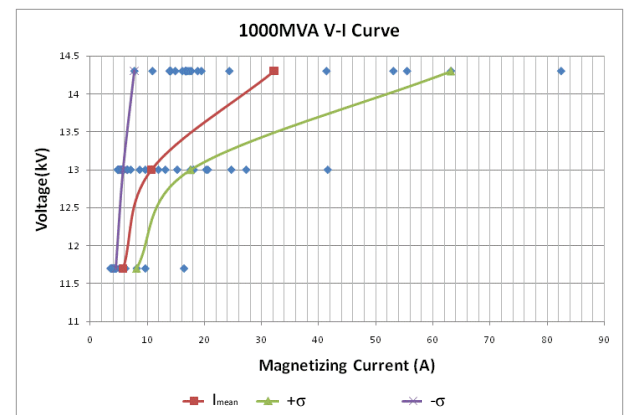


Fig. 5. Mapping open-circuit test data of 1000MVA transformers

III. DESCRIPTION OF MODELLING

A. Simulation Model

The circuit shown in Fig. 1 has been modelled by using ATP software following the implementation described in [7]. The complete simulation circuit is given in Fig. 6. The source impedance was calculated from the short-circuit level of the upstream network. The power transformer (SGT1) was modelled using HYBRID in which the saturation curve was estimated using Frolich equation based on open-circuit test data [12]; the transformer loss at the rated frequency was considered in the model and it is about 0.15% of the total capacity. The double-circuit line represented here was formed by PI circuit [13] which includes the lumped elements of circuit-to-circuit capacitances, ground capacitances, line-to-line capacitances, self resistances, self inductances and mutual inductances. The validation of this simulation circuit was performed in [7].

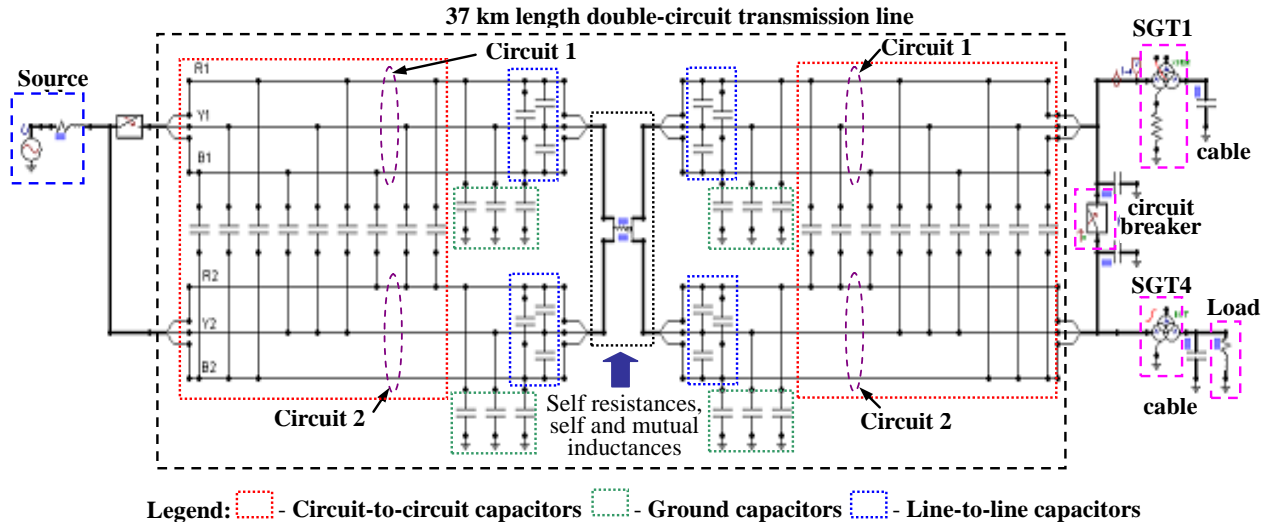


Fig. 6. ATP simulation circuit

B. Parameter Determination

Following the statistical analysis process introduced in section II, 27 scenarios were considered. The results calculated are shown in Table 1 where the mean values and standard deviations of each inter-circuit capacitance are given. As shown in Fig. 7, the element C_{R1R2} in Table 1 represents the capacitance between red phase of circuit 1 and that of circuit 2. Similarly, C_{R1B2} represents the one between red phase of circuit 1 and blue phase of circuit 2. This rule of abbreviation applies to other elements.

The mean value shows that the maximum inter-circuit capacitance is the one between R1 and R2, due to their closest horizontal distance. The minimum one is found to be the one between B1 and R2. Meanwhile, it can be identified that $C_{R1Y2}=C_{Y1R2}$, $C_{R1B2}=C_{B1R2}$ and $C_{Y1B2}=C_{B1Y2}$ due to the symmetric structure.

Based on the C_{mean} and standard deviation σ , the corresponding PDF for each inter-circuit capacitance was calculated, which were also normalized for comparison. Fig. 7 compares the PDFs of C_{R1R2} , C_{R1Y2} and C_{R1B2} . It suggests that C_{R1B2} is least sensitive to geometrical variation, which can also be concluded from the ratio between Standard deviation and arithmetic mean (σ/c_{mean}).

TABLE 1
STATISTICAL ANALYSIS OF INTER-CIRCUIT CAPACITANCES

| Inter-circuit capacitance | $C_{mean}(nF/km)$ | σ (nF/km) | σ / c_{mean} |
|---------------------------|-------------------|------------------|---------------------|
| C_{R1R2} | 1.4135 | 0.0905 | 0.064 |
| C_{R1Y2} | 0.7222 | 0.0836 | 0.116 |
| C_{R1B2} | 0.3336 | 0.0135 | 0.041 |
| C_{Y1R2} | 0.7222 | 0.0836 | 0.116 |
| C_{Y1Y2} | 0.7339 | 0.2415 | 0.329 |
| C_{Y1B2} | 0.5141 | 0.0941 | 0.183 |
| C_{B1R2} | 0.3336 | 0.0135 | 0.041 |
| C_{B1Y2} | 0.5141 | 0.0941 | 0.183 |
| C_{B1B2} | 0.7021 | 0.1297 | 0.185 |

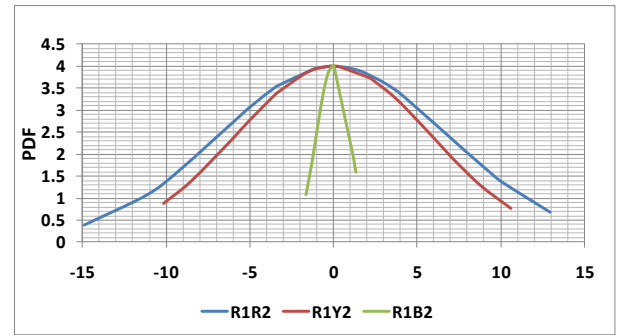


Fig. 7. Normal distribution curves for inter-circuit capacitances

Similarly, the same statistical approach was used to quantify the mean value and standard deviation of transformer magnetizing currents, as shown in Table 2. When the applied voltage is 90% of rated voltage, the ratio between standard deviation and the mean of magnetizing current is small; whereas in the case of 110% of rated voltage, the ratio is high, indicating that the possible range around the knee point region is wider.

TABLE 2
NO-LOAD MAGNETIZING CURRENT EXPRESSED IN -1σ , MEAN AND $+1\sigma$

| 750 MVA transformers | | | |
|-----------------------|---------------|--------------|---------------------|
| Applied Voltage | $T_{mean}(A)$ | σ (A) | σ / T_{mean} |
| 90% | 6.73 | 2.02 | 0.3 |
| 100% | 22.18 | 10.65 | 0.48 |
| 110% | 53.71 | 43.9 | 0.82 |
| 1000 MVA transformers | | | |
| Applied Voltage | $T_{mean}(A)$ | σ (A) | σ / T_{mean} |
| 90% | 5.14 | 2.7 | 0.53 |
| 100% | 11.15 | 8.54 | 0.77 |
| 110% | 30.32 | 29.45 | 0.97 |

IV. CASE STUDY AND RESULT ANALYSIS

A. Simulation Cases

Based on statistical data shown in Table 1 and Table 2, simulations considering various line and transformer combinations were carried out and analysed, with the complete results shown in the appendix. Two typical cases are discussed in detail.

Case I: The line capacitances were fixed at the value corresponding to $C_{\text{mean}} - \sigma$. The impacts of the 750MVA transformer magnetizing curves are considered. The input parameters are the T_{mean} , $T_{\text{mean}} - \sigma$ and $T_{\text{mean}} + \sigma$ of transformer saturation characteristic given in Table 2. The results are shown in Fig. 8 where the columns of blue, red and green are the number of occurrence of FM, SM and DM respectively.

Typical responses of these three modes can be referred to Fig. 9 where the voltage-waveform appearing at the primary side of SGT1 transformer follows the DM, SM and FM mode respectively (note that only phase A is shown here to facilitate the illustration). It can be seen that upon the switching action, the system will undergo a transient period before going into the FM, SM or DM mode. By comparing these three modes, the FM gives sustain overvoltages and therefore is of more concern.

Case II: To assess the impacts of various inter-circuit capacitor networks, the 1000MVA transformer is chosen and its magnetizing characteristic is described by the mean magnetizing curve. The inter-circuit capacitances of the C_{mean} , $C_{\text{mean}} - \sigma$ and $C_{\text{mean}} + \sigma$ according to Table 1 are considered, with results presented in Fig 10.

B. Result Analysis

From the generated results in case I and II, it is found that the DM ferroresonance is more likely to occur than sustained ferroresonance. Since FM is the most destructive case, the fact that DM is the dominating mode is favourable. While for sustained ferroresonance, the chance of encountering FM is lower than that of SM. Certain trends related to sustain ferroresonance modes can be observed from these two case studies. Specifically, in case I, the number of SM can see an increase when the magnetizing curve changes from $-\sigma$ to $+\sigma$. The result further indicates that the SM is sensitive to magnetizing characteristic around the knee point area. However, there was no initiation of FM in case I, which indicates that the FM is unlikely to occur when the inter-circuit coupling is weak, despite the variation of transformer magnetizing characteristics. While in case II, as the inter-circuit capacitances change from $-\sigma$ to $+\sigma$, the likelihood of initiating FM can be increased, so is SM. This could be due to the increased power supply through inter-circuit capacitances.

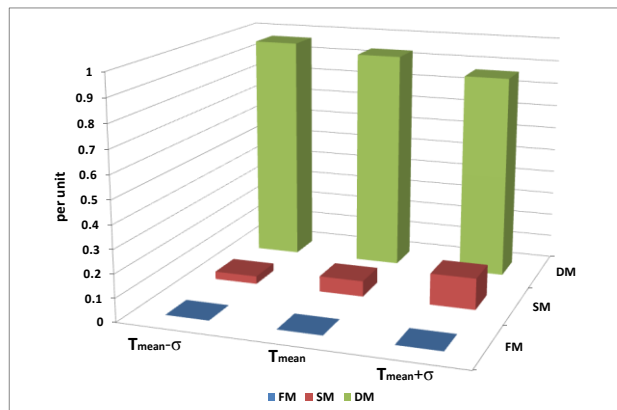
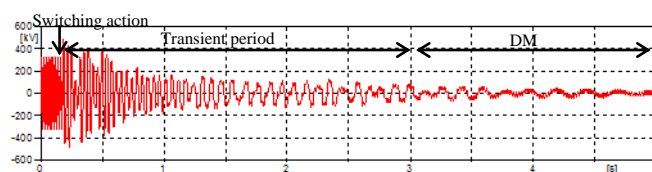
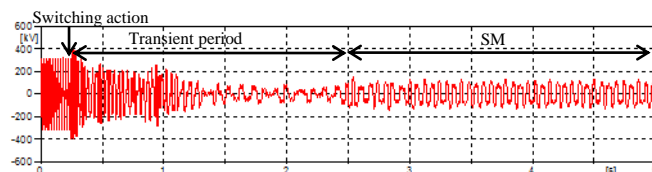


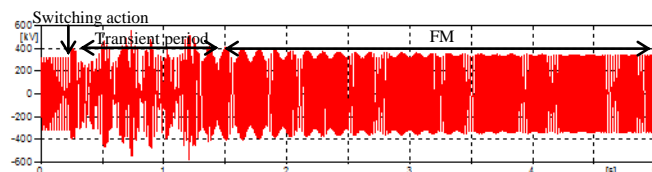
Fig. 8. Results of case I considering variation of transformer saturation characteristic when inter-circuit capacitances are fixed at $C_{\text{mean}} - \sigma$



(a) Transformer terminal voltage waveform of decay mode (DM)



(b) Transformer terminal voltage waveform of sub-harmonic mode (SM)



(c) Transformer terminal voltage waveform of fundamental mode (FM)

Fig. 9. Typical voltage waveforms under DM, FM and SM ferroresonance

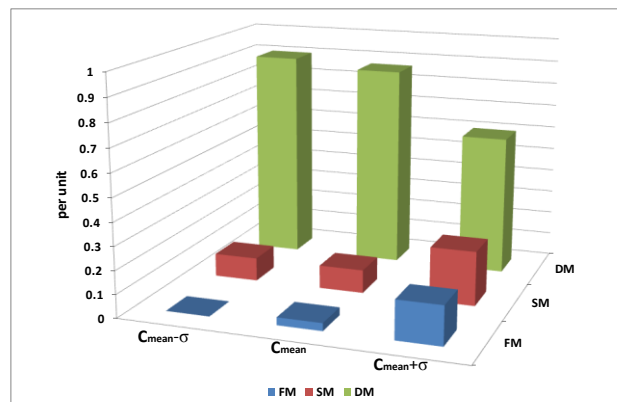


Fig. 10. Results of case II considering variation of inter-circuit capacitances when the magnetizing curve is fixed at T_{mean} of 1000MVA transformer

V. CONCLUSIONS

This paper presents a statistical analysis of ferroresonance phenomena for 400kV double-circuit transmission systems. The circuit parameters have been statistically analyzed, specifically the ranges for inter-circuit coupling capacitances were identified and the variation of transformer magnetizing curves was taken into account. Simulation case studies were performed and the results show that the chance of encountering sustained ferroresonance, if is not the same, does not increased significantly for all the evaluated line and transformer combinations.

VI. ACKNOWLEDGMENT

The authors would like to express their grateful appreciation for the technical and financial support provided by National Grid, UK.

VII. REFERENCES

- [1] GB Seven Year Statement 2010, National Grid, UK: <http://www.nationalgrid.com/uk/Electricity/SYS/current/>.
- [2] R. H. Brierley, A. S. Morched, and T. E. Grainger, "Compact right-of-ways with multi-voltage towers," *IEEE Transactions on Power Delivery*, vol. 6, pp. 1682-1689, 1991.
- [3] Cigre, "Guidelines for Increased Utilization of Existing Overhead Transmission Line", Working Group B2.13, August 2008.
- [4] "Ferroresonance Tests on Brinsworth-Thorpe Marsh 400 kV Circuit," *Technical Report TR(E) 389 Issue 1*, July 2001.
- [5] C. Charalambous, Z.D. Wang, M. Osborne and P. Jarman, "Validation of a power transformer model for ferroresonance with system tests on a 400 kV circuit," *International conference of power system transient 2007*, Lyon, France, 4-7 June 2007.
- [6] E.J. Dolan, D.A. Gillies, E.W. Kimbark, "Ferroresonance in a Transformer Switched with an EHV Line," *IEEE Transactions on Power Apparatus and Systems*, vol.PAS-91, no.3, pp.1273-1280, May 1972.
- [7] S.P. Ang, J.P. Peng, Z.D. Wang, "Identification of key circuit parameters for the initiation of ferroresonance in a 400-kV transmission system," *2010 International Conference on High Voltage Engineering and Application (ICHVE)*, vol., no., pp.73-76, 11-14 Oct. 2010
- [8] P. Ferracci, "Ferroresonance", Groupe Schneider: Cahier technique no 190, <http://www.schneiderelectric.com/en/pdf/ect190.pdf>, pp. 1-28, March 1998.
- [9] "National Grid, UK data sheet, TGN(E)166," February 2002.
- [10] K. Kopsidas, S. M. Rowland, M. N. R. Baharom and I. Cotton, "Power transfer capacity improvements of existing overhead line systems," in *International Symposium on Electrical Insulation (ISEI)*, pp. 1-5.
- [11] M. R. Irvani, A. K. S. Chaudhary, W. J. Giesbrecht, I. E. Hassan, A. J. F. Keri, K. C. Lee, J. A. Martinez, A. S. Morched, B. A. Mork, M. Parniani, A. Sharshar, D. Shirmohammadi, R. A. Walling, and D. A. Woodford, "Modeling and analysis guidelines for slow transients. III. The study of ferroresonance," *IEEE Transactions on Power Delivery*, vol. 15, pp. 255-265, 2000.
- [12] B. Mork, F. Gonzalez, D. Ishchenko, D. Stuehm, and J. Mitra, "Hybrid Transformer Model for Transient Simulation: Part I - Development and Parameters," in *Power Engineering Society General Meeting*, 2007. IEEE, 2007, pp. 1-1.
- [13] ATP Rule Book and Theory Book, EEUG 2007.

VIII. APPENDIX

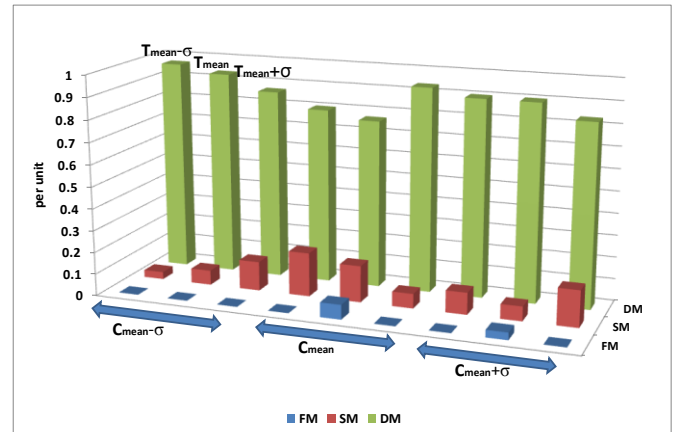


Fig. A1. The frequency of occurrence of ferroresonance with consideration of 750MVA transformer

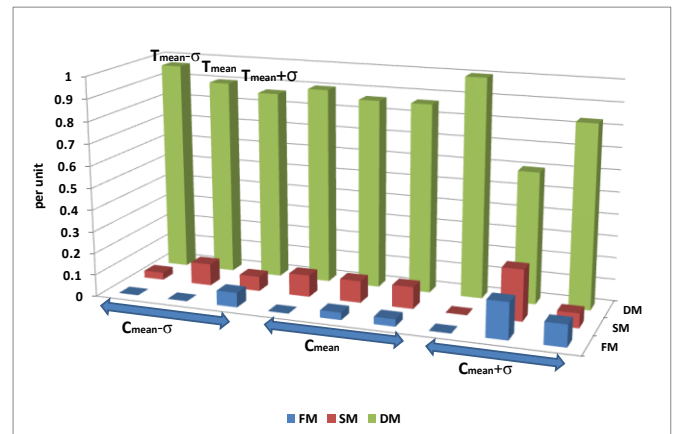


Fig. A2. The frequency of occurrence of ferroresonance with consideration of 1000MVA transformer